

EFFECTIVE STIFFNESS OF A PARTIALLY DEBONDED SPHERICAL PARTICLE

Akihiro WADA *, Yusuke NAGATA **, Shinya MOTOGI ***

* Department of Mechanical Engineering, Kobe City College of Technology

** Interdisciplinary Graduate School of Science and Engineering, Tokyo Institute of Technology

*** Department of Intelligent Materials Engineering, Osaka City University

Keywords: *particulate composite, debonding, effective stiffness, FEM, damage mechanics*

Abstract

In this study, partially debonded spherical particles in a particulate composite are analyzed by three-dimensional finite element method to investigate their load carrying capacities, and the way to replace a debonded particle with an equivalent inclusion is examined. The variation in Young's modulus and Poisson's ratio of a composite with the debonded angle is evaluated for different particle arrangements and particle volume fractions, which in turn compared with the results derived from the equivalent inclusion method. Consequently, it is found that by replacing a debonded particle with an equivalent orthotropic one, the macroscopic behavior of the damaged composite could be reproduced so long as the interaction between neighboring particles is negligible.

1 Introduction

In particulate composites, there are a variety of damage modes such as fracture of particles, interfacial debonding between constituents and cracking in matrix, which lead to the degradation of macroscopic material properties. However, if the damage process could be controlled, the local damage might be available as toughening mechanism due to the energy dissipation[1]. The observed damage modes depend on the mechanical properties of the constituents and the interfacial strength between them. In hard particle reinforced composites, interfacial debonding are most frequently observed mode of damage[2].

In this paper, the unit-cell analysis based on three-dimensional finite element method is performed to investigate the load carrying capacity of a partially debonded particle, and the way to replace the debonded particles to the equivalent

homogeneous inclusions is examined in the framework of the continuum damage mechanics.

2 FEM analysis of particulate composite including debonded particles

2.1 Modeling of a debonded particle

The particle arrangement and the debonding pattern are simplified in order to analyze particulate composites by three-dimensional finite element method. Although the particle arrangement of manufactured composites would have no regularity, in this study it is assumed that all particles are in the arrangement of simple cubic lattice(SC), body-centered cubic lattice(BCC) and face-centered cubic lattice(FCC), respectively. Fig.1 shows the composite of BCC particle arrangement under the uniaxial load ($\sigma=1$). For simplicity, all particles are assumed to be in the same stage of damage process; each particle has the debonding of 2θ on its top and bottom interface perpendicular to the loading axis. The above assumptions make it possible to deal with the overall composite materials as the unit-cell model under the appropriate boundary condition. Although these assumptions are fairly impractical, we used them because the main purpose of this study is to investigate the change in the load carrying capacity of a single spherical particle with debonding.

Considering the periodic particle arrangement in composite, the volume V in Fig.1 is selected as the analytic region for BCC particle arrangement. The meshed view of the volume V is shown in Fig.2, where a and r represent the length on a side of the cubic and radius of the particle respectively. The boundary condition is selected so that the vertical displacements of the three planes which contact the origin equal to 0 as well as the vertical displacements of the other three planes keep the

same value in each plane. Here the volume fraction of particles V_f is represented by the ratio of r to a . The simulation was carried out for three different particles (glass, copper and steel), and four kinds of V_f (0.01, 0.1, 0.2 and 0.3) were used. The material properties of the constituents are summarized in Table 1. The commercially available FEM code ANSYS was used for the analysis and 20 nodes solid element was selected for every calculation.

Table 1 Material properties used in the analysis.

		Young's modulus[GPa]	Poisson's ratio
Matrix	Unsaturated polyester	3	0.37
Particle	Glass	70	0.22
	Copper	124	0.34
	Steel	206	0.30

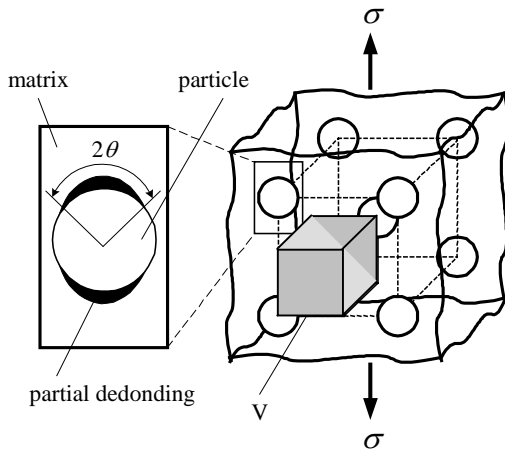


Fig.1 Modeling of random particulate composite as BCC particle arrangement.

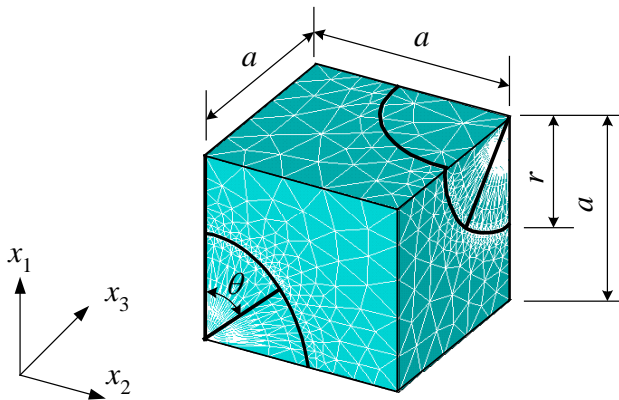


Fig.2 FEM mesh used in the analysis for BCC.

2.2 Analytical results

Figure 3 and 4 show the variation of the macroscopic Young's modulus and Poisson's ratio with the increase of the debonded angle θ . Vertical axes of these figures are normalized by the initial undamaged composite properties. It should be noted that the contact between particles and matrix becomes unignorable for $\theta > 60^\circ$, therefore hereafter we deal with the analytical results for $\theta < 60^\circ$.

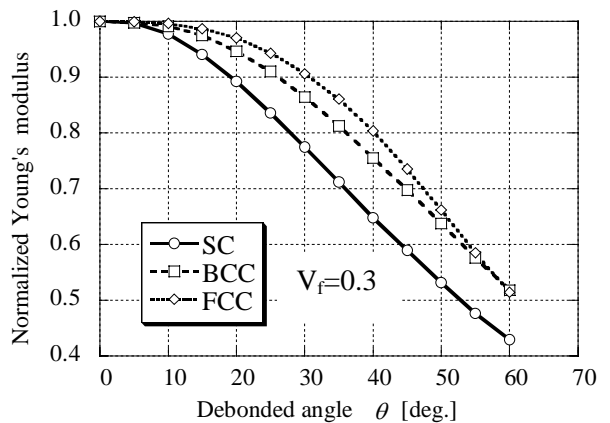
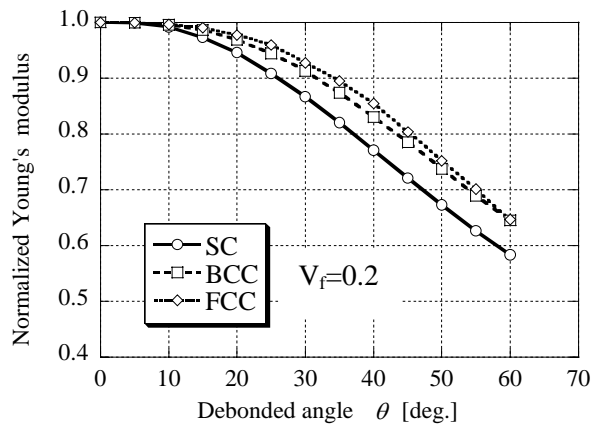
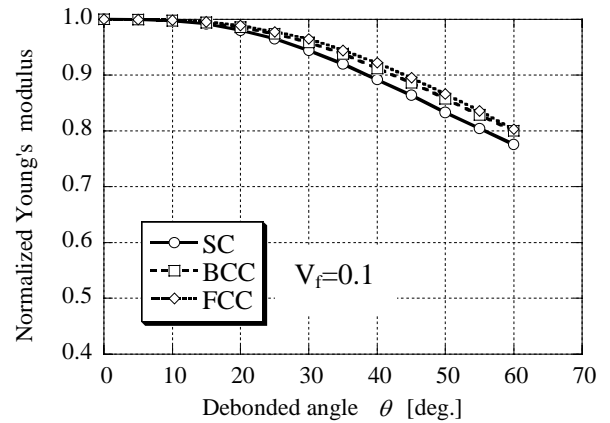


Fig.3 Dependence of Young's modulus of composite on the debonded angle.

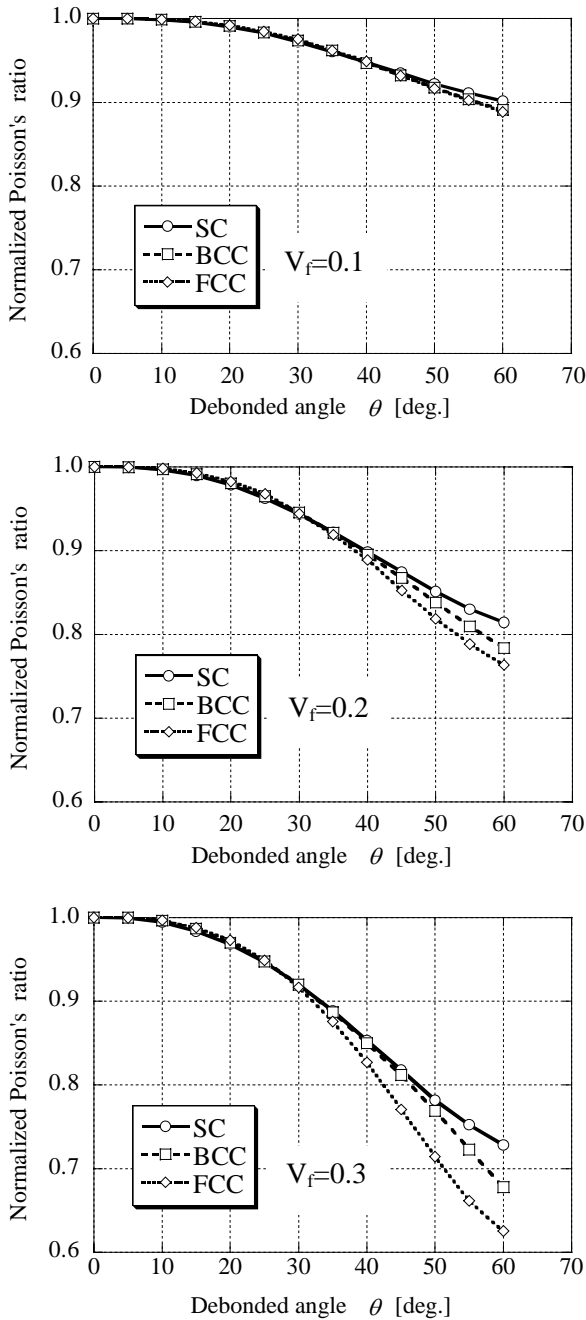


Fig.4 Dependence of Poisson's ratio of composite on the debonded angle.

Although it is possible to define the contact elements on the interface of the debonded particle, for the case of uniaxial tension the mode I component of the stress intensity factor at the front edge of the debonding is negligible for $\theta > 60^\circ$, so that the propagation of the crack over $\theta = 60^\circ$ is impractical. From these figures, it is confirmed that Young's modulus and Poisson's ratio decrease with the increase of the debonded angle for every particle

arrangements, and the variation is more pronounced for higher particle volume fraction, reflecting the increase of the total debonded area. It can be seen also from these figures that the decreasing rate varies with the particle arrangement and are wide-spreading for the case of high particle volume fraction, resulting from the interaction between neighboring particles. In isotropic damage models, the debonded particle is assumed to be replaced by a void of equivalent size, therefore it is impossible to predict gradual development of the internal damage as shown in Fig.3, 4. In this study, to predict the damage behavior of particulate composites more precisely, hereafter we propose the method to replace a debonded particle with an equivalent inclusion.

3 Replacement with equivalent homogeneous inclusions

3.1 Equivalent inclusion method

In this chapter, the stiffness search of an equivalent inclusion is a main target. The search is conducted under the condition that the fictitious composite(Fig.5(b)) can predict similar macroscopic behavior to the composite including partially debonded particles(Fig.5(a)). Since the debonded particles could be treated as orthotropic materials for axisymmetric shape of debondings, there exist nine independent stiffness components for an equivalent particle[3], therefore it is impractical to determine all stiffness components simultaneously. In this study, by introducing the concept of continuum damage mechanics, the stiffness components are represented by three independent variables.

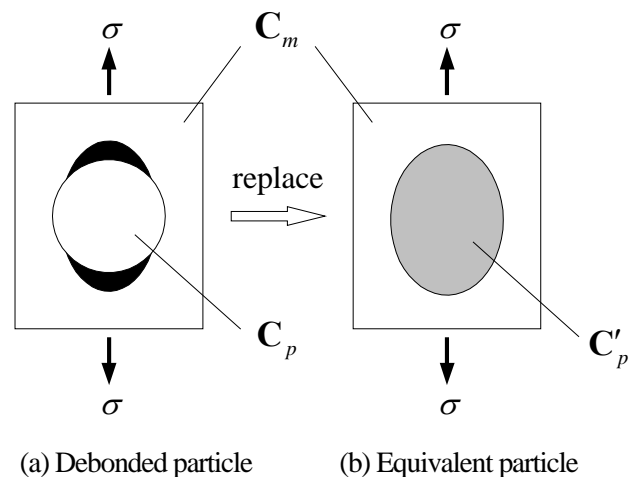


Fig.5 Replacement of a debonded particle with an equivalent particle.

In continuum damage mechanics approach, an averaging technique ignoring fine details is employed to deal with the problem, and the phenomena of progressive material degradation are introduced in the theory by a set of internal state variables (damage variables) under service loading. We could apply an averaging technique to an entire composite to characterize the internal damage process. However, in this paper instead, the averaging technique is applied only to debonded particles. Once the rule of homogenization of a debonded particle is established, we can predict the damage process of an entire composite with the aid of micromechanics[4],[5].

There have been a number of damage mechanics models developed. In this study, the model proposed by Chow & Wang[6] is employed for simplicity. The effective stress of a degraded material is defined by following equation.

$$\boldsymbol{\sigma}' = \mathbf{M}(\mathbf{D})\boldsymbol{\sigma} \quad (1)$$

where $\mathbf{M}(\mathbf{D})$ is tensor of rank four, which they call "damage effect tensor". Introduction of this new tensor leads to the following expression of the effective stiffness.

$$\mathbf{C}' = [\mathbf{M}^T \mathbf{C}^{-1} \mathbf{M}]^{-1} \quad (2)$$

where \mathbf{C} represents the stiffness of the virgin material. $\mathbf{M}(\mathbf{D})$ is proposed by Chow & Wang[6] as follows.

$$[M_{ij}(D)] = \begin{bmatrix} \frac{1}{1-D_1} & 0 & 0 & 0 & 0 & 0 \\ 0 & \frac{1}{1-D_2} & 0 & 0 & 0 & 0 \\ 0 & 0 & \frac{1}{1-D_3} & 0 & 0 & 0 \\ 0 & 0 & 0 & \frac{1}{\sqrt{(1-D_2)(1-D_3)}} & 0 & 0 \\ 0 & 0 & 0 & 0 & \frac{1}{\sqrt{(1-D_2)(1-D_1)}} & 0 \\ 0 & 0 & 0 & 0 & 0 & \frac{1}{\sqrt{(1-D_1)(1-D_3)}} \end{bmatrix} \quad (3)$$

where D_1 , D_2 and D_3 represent damage variables associated with x_1 , x_2 and x_3 axes respectively. Equation(3) gives the framework of material anisotropy, and typical orthotropic damage states can be expressed by this equation.

The application of the above concept to debonding damage of particulate composites lead to the following equation in which \mathbf{C}'_p represents the effective stiffness of a partially debonded particle.

$$\mathbf{C}'_p = [\mathbf{M}^T \mathbf{C}_p^{-1} \mathbf{M}]^{-1} \quad (4)$$

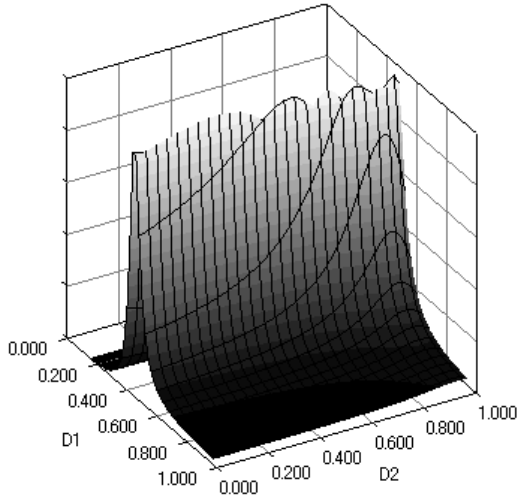
where \mathbf{C}_p represents the stiffness of an intact particle. If x_1 axis is selected parallel to the loading direction, D_1 represents the damage variable along with the loading direction, and D_2 and D_3 are the damage variables perpendicular to the loading direction. It can also be assumed that D_2 always equals to D_3 because of the circular shape of a debonded area in x_2 - x_3 plane. Consequently, a number of damage states can be produced by only two independent variables (D_1 , D_2) along with Eq.(3) and Eq.(4).

3.2 Optimum value search for damage variables

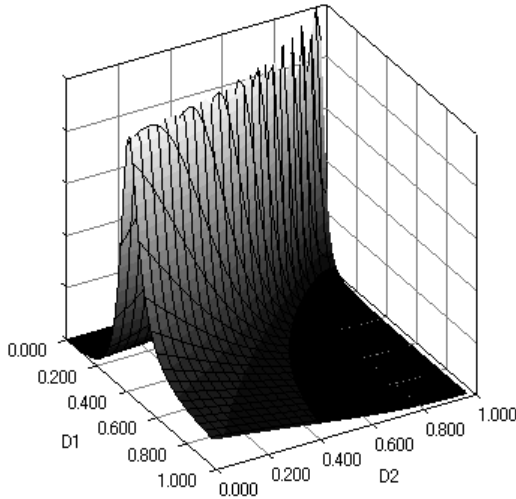
In order to investigate the relationship between the debonded angle and the effective stiffness of the particle, an attempt was made to find out optimum damage variables for respective debonded angle. As has been mentioned in the literature[7], damage variables (D_1 , D_2) range from 0 to 1. Therefore, optimisation is conducted in the following steps.

- ① D_1 and D_2 are selected in 50 patterns respectively at interval of 0.02, then $50 \times 50 = 2500$ patterns of damage state are numerically created.
- ② Effective stiffness of an equivalent inclusion is calculated with selected combination of damage variables (D_1 , D_2) along with Eq.(3) and Eq.(4).
- ③ Fictitious composites including equivalent particles having the above elastic properties is produced by FEM software, then macroscopic Young's modulus and Poisson's ratio are calculated.
- ④ Comparing the macroscopic behaviour between strict analysis and equivalent inclusion method, optimum damage variables are selected.

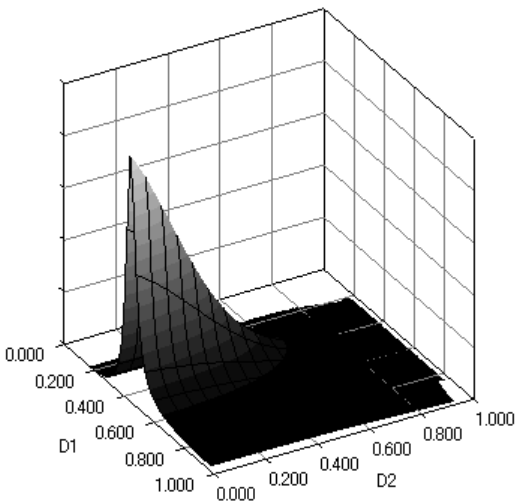
Figure 6 shows the results of the optimum value search for SC particle arrangement at $\theta=30^\circ$, in which z-axis represents the degree of suitability between strict analysis and equivalent inclusion method as shown in Fig.5(a),(b). The degree of suitability is defined by the reciprocal number of the square error between them. Figure 6(a) shows the result for Young's modulus correspondence, and Fig.6(b) shows the result for Poisson's ratio correspondence. Furthermore, Fig. 6(c) shows the



(a) Optimisation for Young's modulus.



(b) Optimisation for Poisson's ratio.



(c) Optimisation for Young's modulus and Poisson's ratio.

Fig.6 Probability plot of damage variables.
(SC, $\theta = 30^\circ$, $V_f = 0.1$)

result based on both of them. In these figures, large value in z-axis means suitable combination of damage variables. The analytical results indicate that selection of the optimum combination of damage variables is difficult for Fig.6(a), (b). Consequently, the consideration of two elastic constants (Young's modulus and Poisson's ratio) is required to identify the best combination with good accuracy.

Over the past few decades, a large number of studies have been made on the damage formulation of composite materials. In these previous models, generally, the comparison of macroscopic stress-strain responses between the experiment and the prediction is made in order to verify the effectiveness of the proposed model. However, as shown in Fig.6(a), there are a number of solution candidates, then verification based on the macroscopic stress-strain response is inadequate to demonstrate the validity of the model. In this study, to avoid the above uncertainty both Young's modulus and Poisson's ratio are taken into consideration in optimum value search of damage variables.

4 Results and discussion

4.1 Effect of particle volume fraction and particle arrangement

To begin with, glass particle dispersed composites are exclusively focused on to investigate the effect of particle volume fraction V_f and particle arrangement on the effective stiffness of a debonded particle. In Fig.7, the optimum combinations of damage variables (D_1 , D_2) for individual debonded angle θ are plotted for each case. From these figures, it is found that D_1 has similar tendency of incrementation for every particle arrangements, although the discrepancy becomes detectable with the increase of V_f . On the other hand, D_2 start to increase around $\theta = 45^\circ$ for $V_f = 0.01, 0.1$, whereas unpredictable results are obtained for $V_f = 0.2, 0.3$. These analytical results indicate that the interaction between neighboring particles become remarkable for higher particle volume fraction. It also should be noted that even in the composite with dilute particle concentrations ($V_f = 0.01, 0.1$) the debonded angle at which D_2 start to increase is delayed in FCC compared to other particle arrangements, which may also be caused by the interaction between neighboring particles. In FCC, the length between neighboring particles is smaller than that of the other

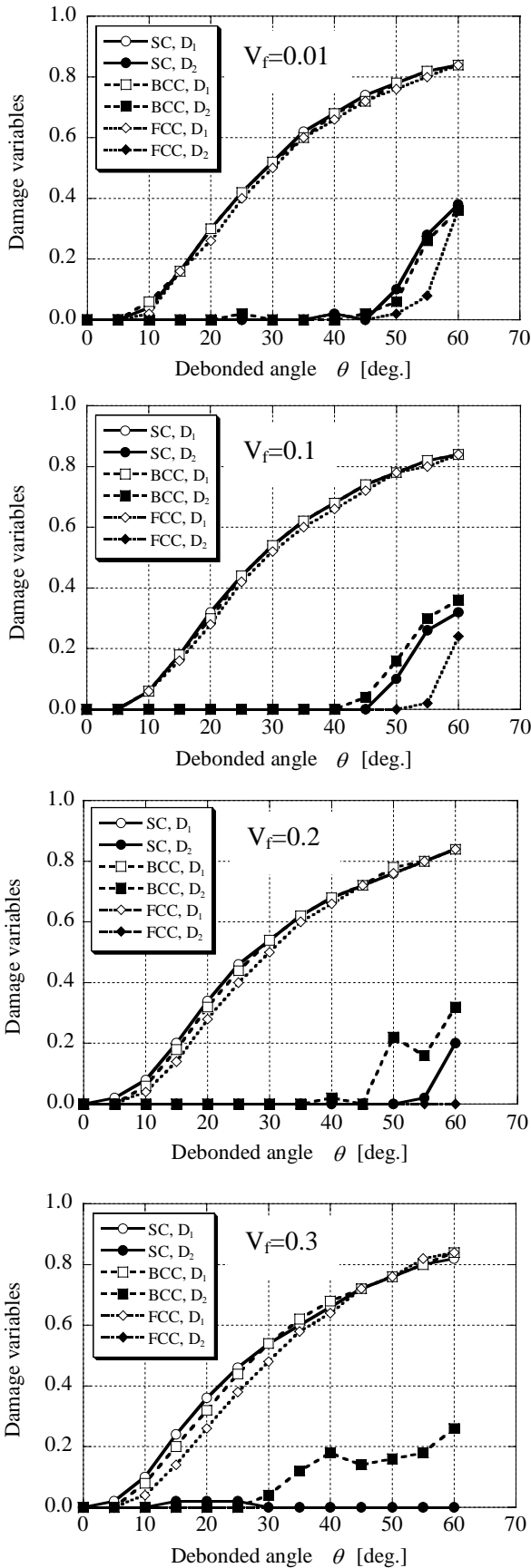


Fig.7 Dependence of damage variables on the debonded angle.

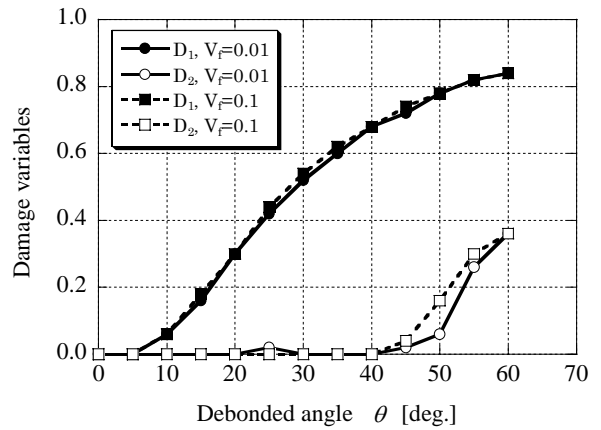


Fig.8 Dependence of damage variables on the debonded angle.(BCC)

particle arrangements at the same particle volume fraction. For instance the ratio of the shortest distance from surface to surface between neighboring particles is SC : BCC : FCC = 1 : 0.96 : 0.81, so that the interference effect is pronounced in FCC.

Figure 8 shows the comparison of optimum damage variables between different particle volume fractions in BCC. Good agreement observed in this figure indicates that particle volume fraction does not have significant effect so long as the interaction between neighboring particles is negligible. Similar rule is also confirmed for other particle arrangements. Consequently, it is concluded that D_1 and D_2 are dependent only on the debonded angle θ , so that the effective stiffness of a debonded particle can be expressed by a function of θ alone in the case of dilute particle concentrations.

4.2 Effect of particle stiffness

Figure 9(a) shows the dependence of damage variables on particle stiffness for dilute particle concentrations ($V_f = 0.01, 0.1$). From these graphs, it is found that the increasing rates of D_1 have similar tendency even if the particle stiffness is different; V_f has little effect for dilute particle concentrations. However it shows clear dependence on particles stiffness, which reflects that stress relaxation is more pronounced for the composite including higher stiffness particles. Figure 10 shows the degradation of composite stiffness with increasing the debonded angle for three different particles at $V_f = 0.3$. Reflecting the particle stiffness shown in Table 1, the stiffness of the intact composite ($\theta = 0^\circ$) is large for steel particles and followed by copper and glass particles. Also it is confirmed that the difference between three particles tends to converge with

debonded angle. This implies that particles carry no longer significant load around $\theta=60^\circ$. Consequently, large difference of the stiffness between constituents cause significant drop in the composite stiffness when debonded. Then, it leads to the accelerating increase of D_1 as shown in Fig. 9(a).

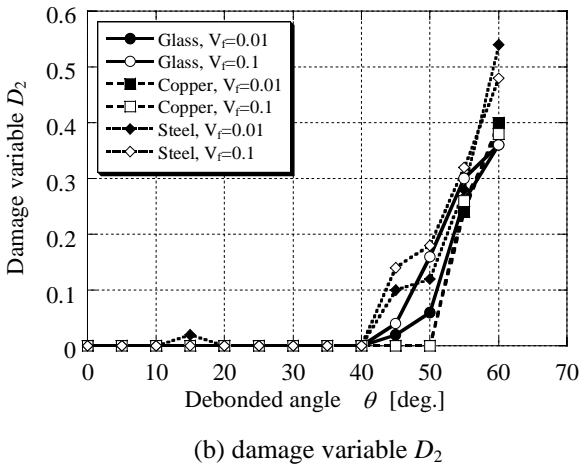
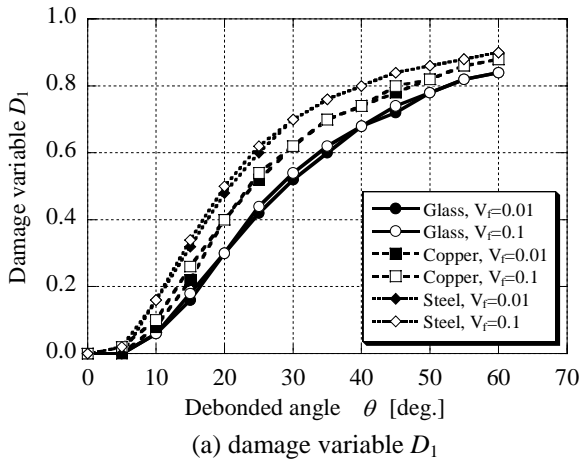


Fig.9 Dependence of damage variables on the debonded angle. (BCC)

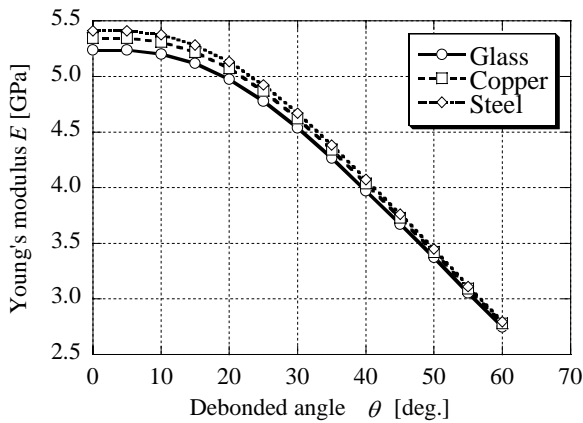


Fig.10 Degradation of Young's modulus of composite with the debonded angle. (BCC, $V_f=0.3$)

In contrast, the dependence of D_2 on particle stiffness seems unclear as shown in Fig.9(b). There observed some scattering of the increasing rate over the debonded angle $\theta=45^\circ$. In order to investigate the observed difference between D_1 and D_2 , probability plot of damage variables for $\theta=45^\circ$ was checked(Fig.11). As shown in Fig.11, the probability is less sensitive to the variation of D_2 than that of D_1 , which lead to the relatively large error for D_2 identification. This is the reason for the observed scattering of D_2 identification, that is D_2 identification might be influenced by the analytical condition such as the number or shape of the elements.

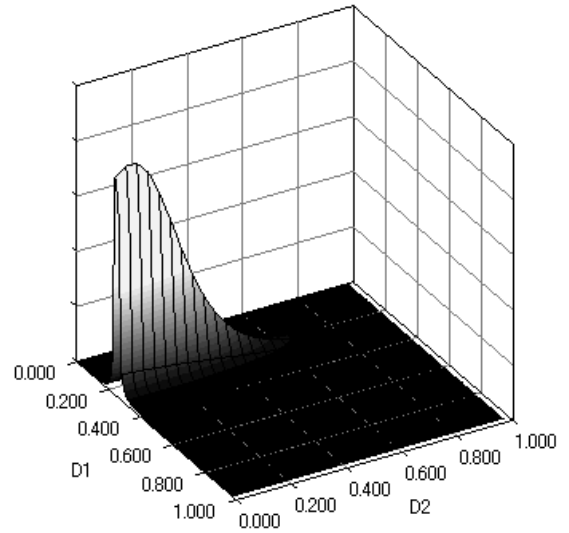


Fig.11 Probability plot of damage variables. (Glass, BCC, $V_f=0.1$, $\theta=45^\circ$)

Next, an attempt is made to formulate the dependence of D_1 on the stiffness ratio between constituents. As shown in Fig.9(a), the increasing rate of D_1 is pronounced when the composite include relatively hard particles. Reminding that damage variables range from 0 to 1, they should converge to 1 at $\theta=90^\circ$ for each type of particle. Now we select the variation of D_1 for glass particles as the master curve of D_1 , and formulate the shift factor reflecting the stiffness ratio between different particles. In order to satisfy boundary condition at $\theta=90^\circ$, the following transformation equation is assumed.

$$D_1 = (D_g)^n \quad (5)$$

where, D_g indicates the damage variable of glass particle, and n is called shift factor.

The shift factor n is proposed as follows.

$$n = f\left(\frac{R_p}{R_g}\right) = f\left(\frac{E_p/E_m}{E_g/E_m}\right) = f\left(\frac{E_p}{E_g}\right) \quad (6)$$

R_g : the stiffness ratio between glass particle and matrix

R_p : the stiffness ratio between the particle under consideration and matrix

E_g : Young's modulus of glass particle

E_p : Young's modulus of the particle under consideration

E_m : Young's modulus of matrix

Following to Eq.(6) , if the same matrix is used, the shift factor n is dependent only on the stiffness ratio between different particles.

In order to find out the optimum shift factor n for copper and steel particles, comparisons were made between strict analysis(Fig.9(a)) and predictions derived from Eq.(5). Figure 12 shows the optimum shift factor for different stiffness ratio(E_p/E_g). The shift factor is found to have linear dependence on the stiffness ratio between particles. The following is the approximated equation for n . It should be noted that the maximum error of Eq.(7) is less than 2%.

$$n = f(E_p / E_g) = 0.353 \cdot \left(\frac{E_p}{E_g}\right) + 0.662 \quad (7)$$

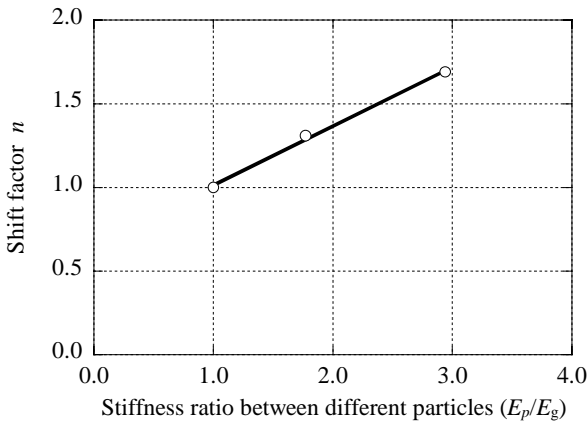


Fig.12 Relationship between shift factor n and stiffness ratio between particles. (BCC, $V_f=0.1$)

In Fig. 13, the comparison of damage variables is made between different particles, where the curves of copper and steel particles are shifted based on Eq.(5),(7). There observed excellent agreement, so the master curve of D_1 is obtained. Consequently, the difference of particle stiffness can be formulated through Eq.(5),(7).

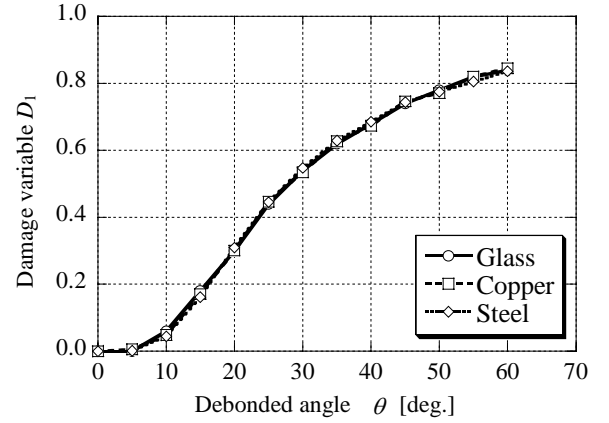


Fig.13 Master curve of damage variable D_1 (BCC, $V_f=0.1$). Shift factor $n=1.31$ for copper, $n=1.69$ for steel.

4.3 Comparison between strict analysis and equivalent inclusion method

As has been mentioned, a debonded particle can be replaced by an equivalent homogeneous inclusion, and damage variables(D_1 , D_2) of the particle can be expressed by a function of θ alone so long as the interaction between neighboring particles is ignorable. Now, we try to extend the above concept to relatively large concentration of the particles. Strictly speaking, the replacement of the debonded particles to equivalent inclusions is inappropriate for $V_f > 0.1$. However, as shown in Fig.7, D_1 is insensitive to V_f , and D_2 , which is significantly altered by V_f , has wide range of appropriate value for each debonded angle(Fig.11). Therefore, we can approximately use Fig.8 for wide range of particle concentration.

Figure 14,15 show the comparisons between strict analysis(Fig.3,4) and equivalent inclusion method based on dilute particle concentration. The approximate calculations are conducted using damage variables for SC particle arrangement ($V_f=0.01$). From these graphs, it was found that the correlations between different analytical methods are fairly good for $V_f=0.1$ and acceptable for $V_f=0.3$. Therefore the equivalent inclusion method presented in this paper can be applied for wide range of particle concentration.

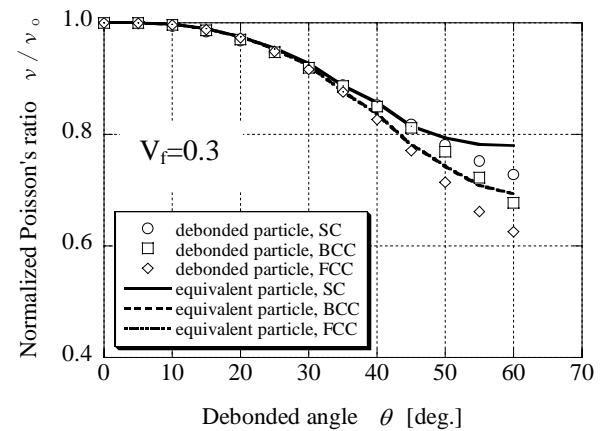
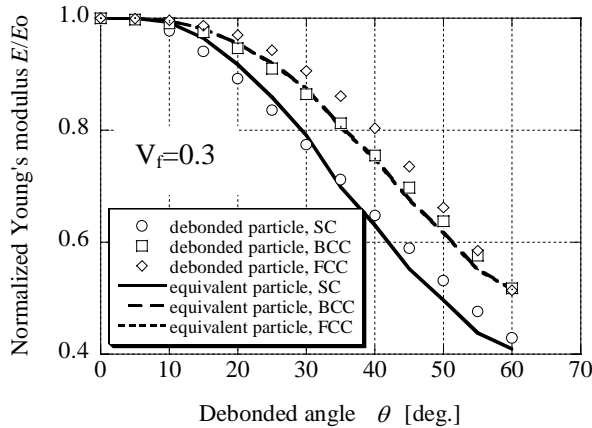
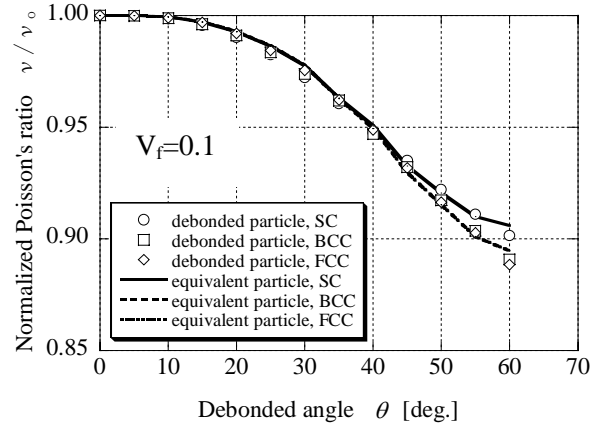
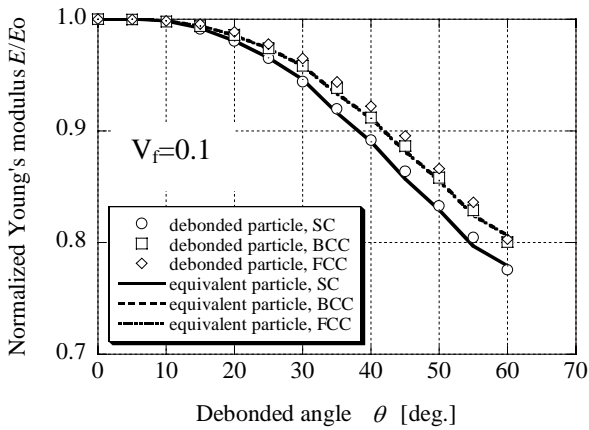


Fig.14 Comparisons of Young's modulus between different analytical methods.

Fig.15 Comparisons of Poisson's ratio between different analytical methods.

5 Conclusion

The unit-cell analysis based on three-dimensional finite element method is performed to investigate the effective stiffness of a partially debonded spherical particle. It was found that by replacing a debonded particle with an equivalent orthotropic one, the macroscopic behavior of the damaged composite could be reproduced so long as the interaction between neighboring particles is negligible. Also the effective stiffness of a particle is derived as a function of the debonded angle in the framework of continuum damage mechanics. It was also found that the increasing profile of damage variable D_1 can be formulated based on the stiffness ratio of the constituents, and damage variable D_2 is relatively insensitive to particle stiffness. Although the present model is for the composite with dilute particle concentrations, it could approximately be used to predict the macroscopic behavior of general particulate composites.

References

- [1] K. Tohgo, N. Suzuki and H. Ishii, *Int. J. Damage Mech.*, **5** (1996), 150-170.
- [2] A. Wada and S. Motogi, *Materials Science Research International - Special Technical Publication*, **2** (2001), 276.
- [3] R.M.Jones, *Mechanics of composite materials second edition*, Taylor&Francis, Philadelphia (1999).
- [4] J. D. Eshelby, *Proc. R. Soc.*, **A241** (1957), 376-396.
- [5] T. Mori and K. Tanaka, *Acta Met.*, **21** (1973), 571-574.
- [6] C. L. Chow and J. Wang, *Int. J. Fract.*, **33** (1987), 3-16.
- [7] S. Murakami, *J. Applied Mech.* **55**(1988), 280-286.